Nuclear Inst, and Methods in Physics Research B 432 (2018) 42–47

Contents lists available at ScienceDirect

Nuclear Inst. and Methods in Physics Research B

journal homepage: www.elsevier.com/locate/nimb

# A new methodology for studying neutron absorber materials: First results with boron carbide

L. Desgranges[a,*], J.M. Escleine[a], Ph. Bienvenu[a], I. Roure[a], D. Gosset[b], R. Boffy[c], U. Köster[c]

[a] CEA, DEN, DEC F-13108, Saint Paul lez Durance Cedex, France
[b] CEA, DEN, DMN, Université Paris-Saclay, F-91191 Gif-sur-Yvette Cedex, France
[c] Institut Laue-Langevin, 71 Avenue des Martyrs, B.P. 156, 38042 Grenoble Cedex, France

ARTICLE INFO

*Keywords:*
Neutron irradiation
Neutron absorber
Nuclear material
Irradiation design

ABSTRACT

This paper presents a new methodology used to study transmutation damage in boron carbide ($B_4C$). $B_4C$ samples were set in a specially designed sample holder and irradiated in a neutron thermal flux in the ILL reactor. After describing the sample holder and the irradiation conditions, this paper discusses the results of the first post-irradiation examinations by secondary-ion mass spectrometry (SIMS), X-ray diffraction (XRD) and scanning electron microscopy (SEM). The results obtained for a $B_4C$ disc with natural boron composition prove the efficiency of the methodology.

## 1. Introduction

In the nuclear field, there is an increasing demand for more physically based modelling of material properties. The reason for this is twofold: to limit the number of validation irradiations required in real reactor conditions, and to provide more reliable predictions outside the validation domain. This tendency largely applies to nuclear fuel, with numerous papers moving from first-principle calculations to fuel microstructure modelling [1]. This demand for physically based modelling is also relevant for neutron absorber materials, though less work has been done in this field. Boron carbide is one of the most frequently used materials for neutron absorbers and its phenomenology under irradiation has been long documented [2,3]. In actual reactor conditions, it is subjected to both atomic collision with fast neutrons and transmutation reactions due to neutron capture by $^{10}B$ isotopes. Neutron atomic collisions produce collision cascades that result in point or extended defects. $^{10}B$ transmutation reactions (up to $10^{22}\,cm^{-3}$, i.e. about 10% of the total boron in current fast reactor conditions) produce He and Li recoils that induce defects during their stopping and chemical modification of the pristine boron carbide. Helium clusters in over-pressurized small bubbles could lead to inter- and intragranular cracking [4]. The fate of lithium is less clear since this element is not visible using classical methods such as electron probe micro analysis (EMPA) or X-ray photoelectron spectroscopy (XPS).

Physically based modelling requires the identification of each physical mechanism that is needed to describe the material. In the case of boron carbide under irradiation, the effects of atomic collisions with fast neutrons and transmutation reactions cannot be easily separated from the available experimental results obtained by irradiation in nuclear reactors or by ion implantation experiments. During irradiation in a reactor, the material is subjected to a broad neutron energy spectrum leading to a complex weighting of the two interactions, i.e. absorption and ballistic damage. Thus, ballistic and transmutation effects are intricately linked. With ion implantation, a specific irradiation defect can be reproduced by choosing a suitable ion and energy level, but this type of experiment cannot be used to reproduce the transmutation phenomenon as a whole.

Each mechanism also has to be characterised as a function of temperature but samples are required to do this. They must be irradiated at a constant temperature and they must be large enough so post-irradiation characterisation tests can be performed. In reactor irradiation conditions, the temperature follows a complex history as a function of the reactor power and varies spatially as a function of the neutron flux. In ion implantation experiments, the temperature may be known with better accuracy but the resulting irradiated area is usually only a layer less than 1 μm thick. In this case, only a few experimental methods (e.g. TEM) can provide valuable information; X-ray diffraction cannot be used in this instance.

In order to overcome these difficulties, we developed a new methodology for studying neutron absorber materials in which only transmutation defects are produced within bulk samples at a practically constant temperature. This methodology was used for the irradiation of

* Corresponding author.
*E-mail address:* lionel.desgranges@cea.fr (L. Desgranges).

https://doi.org/10.1016/j.nimb.2018.07.011
Received 27 September 2017; Received in revised form 3 July 2018; Accepted 12 July 2018
Available online 21 July 2018
0168-583X/ 

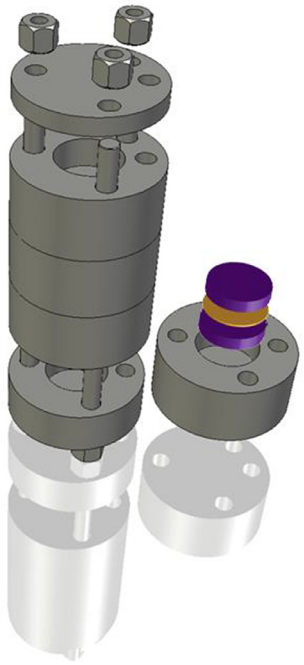

**Fig. 1.** $B_4C$ sample (orange) sandwiched between two SiC discs (purple) positioned in their sample holder (grey). (For interpretation of the references to colour in this figure legend, the reader is referred to the web version of this article.)

$B_4C$ discs in a new sample holder in the high flux reactor at the Institut Laue Langevin (ILL). This paper first describes the sample holder, before detailing the irradiation experiment and the preliminary characterisation results. These results are discussed in the conclusion, showing how the new methodology met our requirements.

## 2. Sample holder

The samples were first settled in an aluminium shuttle so they could fit into the T4 beam tube. A new sample holder was designed not only to meet the above irradiation objectives presented, but also to fit into this shuttle. A schematic diagram of this sample holder is given in Fig. 1.

The $B_4C$ discs were 0.3 mm thick and 10 mm in diameter. They were prepared from a high-density (> 98% of theoretical density = 2.52) pellet with a small grain size (5–10 μm) and mirror-polished surfaces. Two β-SiC discs – 2 mm thick and 10 mm in diameter – were placed on each side of the $B_4C$ discs. These β-SiC (theoretical density = 3.51) discs were prepared from a CVD-made ceramic pellet and were placed in contact with the mirror-polished surface of the $B_4C$ samples. Each SiC-$B_4C$-SiC sandwich was placed inside a hole drilled in an aluminium disc. Five aluminium discs were fabricated and stacked on top of each other to build the sample holder. The $^{10}B$ enrichment of the samples was natural (19.9%) for the three bottom $B_4C$ discs, 48% for the fourth disc and 90% for the top disc. The aluminium discs were held together by three screws. An additional hole was drilled through all the discs to let the air flow out when the sample holder was placed in the capsule. Small zirconium foils were inserted in this hole at different heights to determine the neutron flux using post-irradiation gamma spectrometry. Fig. 2 shows how the sample holder was assembled (Fig. 2a) and its installation in the capsule (Fig. 2b).

This design also guarantees the safe irradiation of the sample holder inside the capsule in the T4 tube. The high thermal conductivity of SiC and the level of contact between the mirror-polished surfaces of $B_4C$ and SiC ensures that the heat produced by the transmutation reactions is removed efficiently. The irradiation time was also set to 5 days, not only to produce a sufficient level of transmutation for further characterisation, but also to minimise the helium production and maintain the pressure increase in the capsule at less than one atmosphere, assuming the total release of helium.

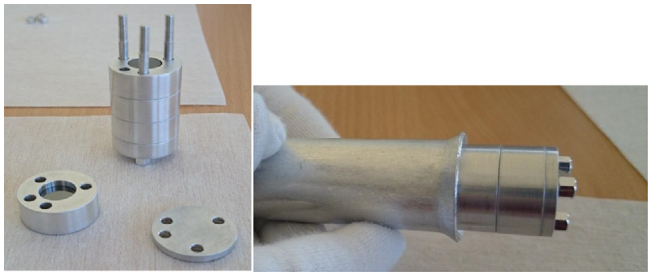

**Fig. 2.** Sample holder fabrication and installation in the aluminium capsule.

## 3. Irradiation

The T4 irradiation tube was positioned in the reflecting light water vessel, very close to the heavy water tank in the ILL reactor. This location leads to a neutron flux with a Maxwellian distribution at a temperature about 20 °C (calculated in reference [5]).

The shuttle was positioned vertically in the T4 tube so that the $B_4C$ discs were parallel to the neutron flux from the core. Unfortunately, the position of the sample holder inside T4 could not be known. As a consequence, the relative position of the zirconium foils (ϕ1) and the SIMS quantitative line scan (ϕ2, discussed below) were not known relative the neutron flux. This neutron flux is known for its large local variations because of nuclear reactions with $^{10}B$ that reduce the flux in the vicinity of the B4C disc. Not knowing ϕ1 and ϕ2 induces large uncertainties in the neutron flux at the positions of the zirconium foils and SIMS line scan. Consequently, we did not attempt to model the neutron flux theoretically but instead chose to rely on its experimental determination.

The penetration depth of 0.025 eV thermal neutrons in natural $B_4C$ is about 130 μm ($\sigma\mathbf{N} = 76\,cm^{-1}$). Thus, the irradiation damage was more or less homogeneous in our 300 μm thick $B_4C$ discs that had natural $^{10}B$ enrichment, despite the local neutron flux changes discussed above.

The capsule containing the sample holder and the five SiC-$B_4C$-SiC sandwiches was irradiated for five days in June 2015. Because of the radiation level of the capsule after irradiation, it was only removed from the hot cell in September 2015. First of all, the two ends of the capsule were cut and the small zirconium foils were removed from the hole drilled for air flow. Gamma spectrometry measurements were used to determine their accumulated dose and the neutron flux during irradiation at different heights inside the sample holder (see Table 1). The average measured flux was consistent with the nominal flux in T4 [6].

Secondly, the capsule was sent to the CEA/Cadarache centre. Its dose rate measured at a distance of 5 cm was 1500 μSv/h after a period of 40 days following the end of the irradiation. This was mainly due to the activation of chromium, which is used as alloying element in the aluminium sample holder and capsule. The capsule was dismantled in a controlled area so the SiC-$B_4C$-SiC sandwiches could be removed. The radioactivity of the SiC and $B_4C$ discs was measured. The dose rate for each sample was less than 0.1 μSv/h at a distance of 5 cm and the labile contamination was less than $0.4\,Bq\,cm^{-2}$ for alpha activity and

**Table 1**
Calculated neutron flux at the different zirconium foil positions.

| Foil number | ❶ | ❷ | ❸ | ❹ | Average |
|---|---|---|---|---|---|
| Foil mass (mg) | 1.59 | 1.63 | 1.71 | 1.35 | |
| Calculated flux in $10^{13}$ n/cm$^2$/s | 1.8 | 1.73 | 1.39 | 2.18 | 1.7 ± 0.3 |

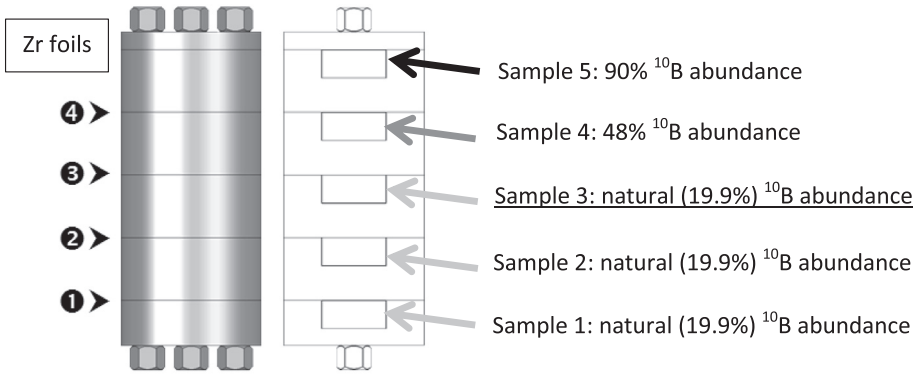


**Fig. 3.** Position of the zirconium flux monitor foils and $^{10}$B enrichment of the samples. NB: Sample 3 was used for further characterisation after irradiation.

4 Bq cm$^{-2}$ for beta activity. This low level of radioactivity (i.e. no classification) made it possible to handle the samples in regular facilities without any major limitations due to radioactivity.

## 4. First characterisations

The sandwich with natural boron located in the middle of the capsule (labelled sample 3 in Fig. 3) was chosen for further analysis. The two SiC discs were separated from the $B_4C$ sample. The $B_4C$ sample and one SiC disc were placed on standard SEM 12.7 mm (1/2″) pin stubs for further analysis by SIMS and XRD. Preliminary SEM analysis showed that a surface film, a few hundred nanometres thick, had been removed from some parts of the $B_4C$ disc. This film is likely to be fabrication pollution due to a small fraction of graphite present in the material (free carbon during the elaboration process). The following section mainly focuses on the behaviour of bulk $B_4C$.

## 5. $B_4C$ sample

The $B_4C$ disc was first characterised by SIMS to evidence the change in isotopic composition induced by irradiation, and secondly by SEM and XRD to evidence the defects created by $^{10}$B transmutation.

SIMS analyses were performed using a positive oxygen primary beam of 4.5 keV to measure positive secondary ions. SIMS depth profiles were performed for $^{10}$B, $^{11}$B and $^{12}$C, which existed before irradiation. They were also performed for $^{7}$Li, which was created during irradiation. The SIMS signal was not proportional to the isotope concentration; it also depended on the ionization yield. Thus, these depth profiles could not be compared quantitatively with each other.

Isotopic depth profiles were performed at different points on the $B_4C$ surface. They all evidenced two regions with different detection yields for B, C and Li ions: one region was situated near the surface while the other was in the bulk (Fig. 4). The SIMS crater depth was measured to be around 1 µm. This confirms that the first region is a few hundred nanometres thick and that it is related to the graphite film mentioned above.

It can be seen that the B and C profiles are flat for sputtering times exceeding 700 s (corresponding to the bulk sample), which is coherent with the neutron absorption length in $B_4C$ with natural $^{10}$B (130 µm); there is no significant change in the transmutation range over a 1 µm depth. In contrast, the lithium profile increases during this timeframe, which implies that the lithium created by transmutation reactions moved out of the $B_4C$ bulk. $^{7}$Li is produced as a recoil atom created during $^{10}$B transmutation; its recoil energy enables it to move a few µm away from its creation place. Recoil implantation in SiC (see later) is then consistent with Li depletion in $B_4C$. Nonetheless, the peak at around 400 s in the lithium profile (see Fig. 5) is a likely sign for Li accumulation, suggesting that Li desorption out of $B_4C$ should also be considered [7]. This peak could also be correlated with small particles that were evidenced by SEM on the $B_4C$ surface. These particles are spheroid in shape; they are deposited on the surface, either isolated or forming clusters (Fig. 6). The dismantling procedure made sure to avoid contamination deposition on the samples, and these spheroids could have been created during irradiation at ILL. We need to better characterise these spheroids to improve our understanding of Li behaviour.

The $^{10}$B/$^{11}$B ratio was also determined quantitatively. For this reason, the surface film was first sputtered to perform measurements in the bulk where the $^{10}$B and $^{11}$B concentrations are constant (Fig. 5). Ten equidistant measuring points were chosen along a 2 mm long line on the disc surface.

The measured $^{10}$B/$^{11}$B ratio was corrected for the experimental isotopic drift using a $B_4C$ reference with a known $^{11}$B composition. The corrected $^{10}$B/$^{11}$B ratio was 0.2529 with a standard deviation of about 1%. This value is significantly lower and more dispersed than the 0.2645 obtained with a standard deviation of 0.3% measured on unirradiated $B_4C$ from the same fabrication batch, which confirms that significant transmutation occurred. Moreover, the higher standard deviation for irradiated $B_4C$ can be attributed to a variation in the $^{10}$B/$^{11}$B ratio that decreases along the disc radius (Fig. 7), consistently with a continuous decrease in the neutron flux in the $B_4C$ disc in the direction escaping the reactor core (see Fig. 4).

X-ray diffraction was performed using Cu K$\alpha_1$ radiation on an asymmetric goniometer. The primary beam (width 100 µm) hit the sample surface at a fixed angle of 2°. This small angle diffraction set-up was chosen to limit the penetration of X-rays inside the $B_4C$ sample because $B_4C$ is a low Z material [8]. The estimated penetration depth of the X-rays in our small-angle diffraction set-up (incidence angle i = 2°) was about 60 µm ($\mu/\sin(i)$ = 170 cm$^{-1}$). As a result, the material analysed by XRD can be considered as homogeneous, apart the pollution surface layer discussed above.

The XRD diffraction diagram of the irradiated $B_4C$ was compared with the reference in Fig. 8. Peak shifts and changes in peak intensity can be clearly identified, showing that the stopping of He and Li produced by transmutation damaged the crystalline structure of B4C. The small fraction of graphite present in the material (free carbon resulting from the elaboration process) shows a significant decrease after irradiation due to disorder or partial amorphisation. A further interpretation of the XRD data using Rietveld analysis is currently in progress.

## 6. SiC sample

The side of one SiC disc in contact with the previously characterised $B_4C$ (sample 3) was also characterised by SIMS and XRD in a manner similar to $B_4C$.

The SIMS depth profile also evidenced an altered near-surface layer (Fig. 9). We assumed this to be the same layer as that previously observed on $B_4C$ partially bonded to the SiC disc. The $^{7}$Li profile evidenced that Li was implanted in SiC with a decreasing intensity towards the SiC

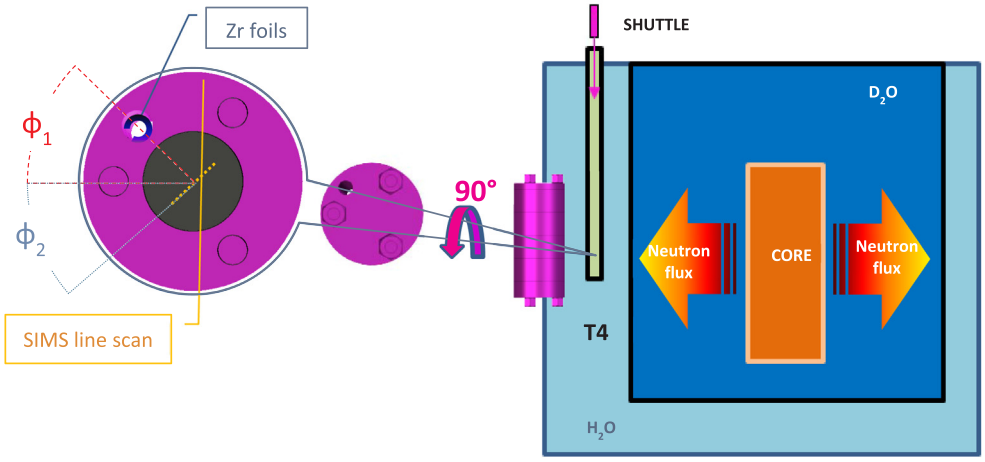


**Fig. 4.** Layout of the T4 tube inside the ILL reactor (left) and position of the sample holder relative to the neutron flux.

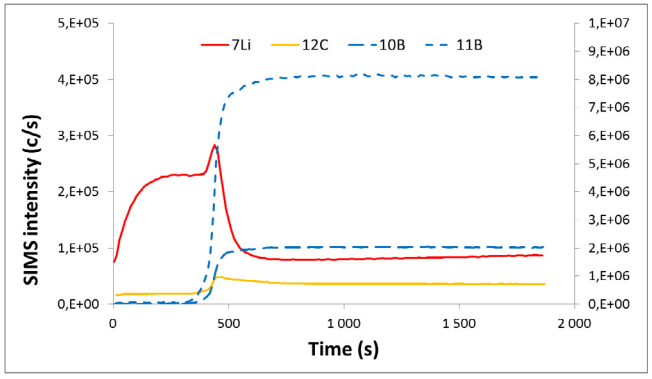


**Fig. 5.** Depth profiles of $^{12}C$, $^{10}B$, $^{11}B$ and $^{7}Li$ obtained by SIMS in the $B_4C$ sample (the scale for the dashed lines is on the left, the scale for the solid lines is on the right).

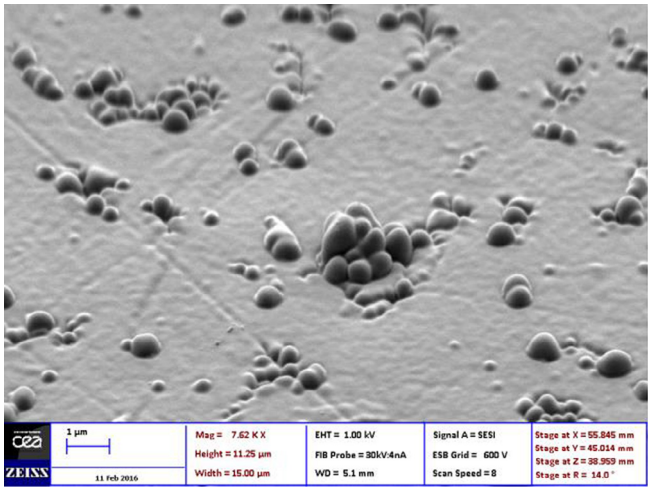


**Fig. 6.** Spheroid particles at the surface of the $B_4C$ disc.

bulk. This decrease is consistent with the implantation of Li recoil atoms because the implantation depth of lithium can be estimated at around a few micrometres and the SIMS crater depth was measured by profilometry at around 0.8 µm.

Fig. 10 shows the XRD pattern for the reference material and irradiated SiC. The irradiated SiC was measured on the side in contact with $B_4C$ during irradiation. This figure evidences the formation of damage in the SiC that appears through peak broadening, intensity change and shifting.

## 7. Discussion

The purpose of this irradiation experiment was to obtain $B_4C$ samples in which only transmutation defects were produced in the bulk at a given temperature. The results discussed in this paper confirm the fact that our objective was reached.

First, the very pure thermal neutron flux in T4 induced no damage due to neutron collisions with atoms in the $B_4C$ samples because the energy transferred by neutron collisions to a B or C atom was less than its displacement threshold. Moreover, the neutron absorption cross-section for the reaction was very high (3840 barns):

$$^{10}B + n \rightarrow {}^{7}Li + {}^{4}He \quad (1)$$

Therefore, only transmutation-induced defects were created: chemical modification, ions slowing down (mainly electronic interactions with the matrix) and nuclear stopping (partly ballistic damage).

The transmutation dose can be determined using two different methods; the first uses the dose rate measured on the zirconium foils, while other uses SIMS results. First, the dose rate measured on the zirconium foils was used to calculate the neutron flux during irradiation: it was evaluated at around $1.8{\cdot}10^{13}$ n cm$^{-2}$ s$^{-1}$. This neutron flux was then used to calculate the transmutation rate in the $B_4C$ sample. This transmutation rate was finally integrated over the duration of the irradiation to obtain the total transmutation yield. This led to about $6{\cdot}10^{20}$ neutron captures/cm$^3$, which corresponds to a 3.4% transmutation yield of $^{10}B$ and 0.6% burn-up of total boron. Second, the $^{10}B/^{11}B$ ratio measured by SIMS before and after irradiation was also used to evaluate the fraction of $^{10}B$ that underwent transmutation; a concentration of about $9{\cdot}10^{20}$ neutron captures/cm$^3$ was deduced, which corresponds to a 4.4% transmutation rate of $^{10}B$. These two evaluations produced roughly consistent results regarding the experimental uncertainties. The preliminary tests carried out to determine the Li concentration by SIMS were also consistent with these evaluations. Referring to literature, a transmutation dose of $10^{21}$ neutron captures/cm$^3$ corresponds to the dose at which irradiation effects have a noticeable effect on the material properties, such as structural damage or helium bubble formation at high temperature. Higher doses were reached in $^{10}B$-enriched samples which were also irradiated.

The irradiation temperature was conservatively evaluated before irradiation to be below 600 °C. However, as this is a very relative estimate due to the local neutron flux changes, we therefore planned to deduce the irradiation temperature from the post-examination of SiC discs in contact with the $B_4C$ samples. SiC samples do not react with thermal neutrons but they can be damaged by transmutation recoils produced near the $B_4C$ surface. $^{7}Li$ and $^{4}He$ created by reaction (1) have recoil energies of 0.84 MeV (94%), 1.01 MeV (6%) for $^{7}Li$ and 1.47 MeV

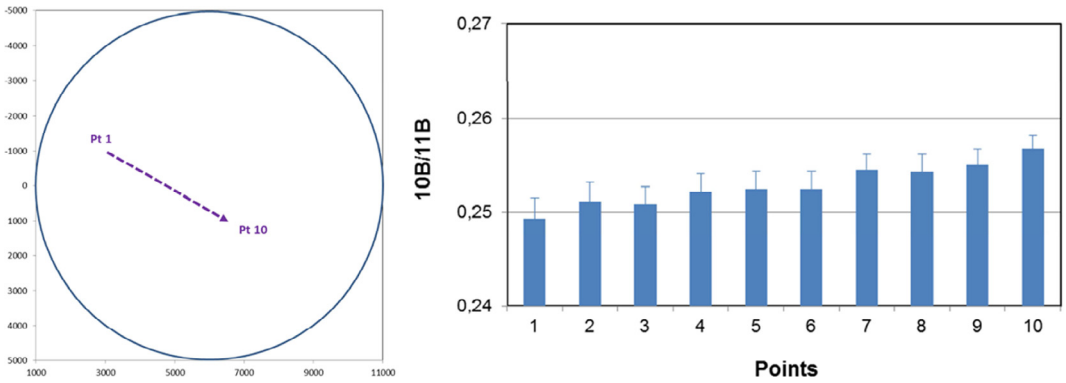


**Fig. 7.** $^{10}B/^{11}B$ measured isotopic ratio along the 2 mm long dashed line of the $B_4C$ disc after removal of the surface film.

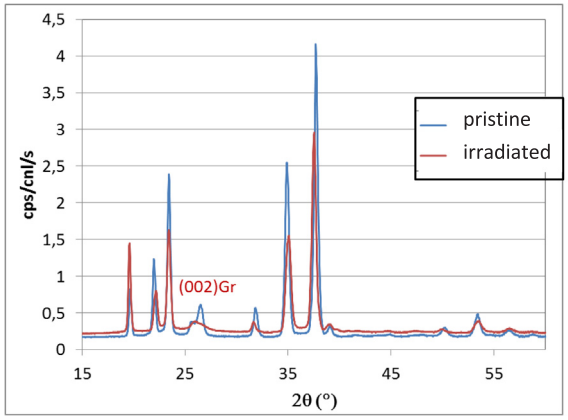


**Fig. 8.** X-ray diffraction diagrams before (blue) and after (red) irradiation. The (0 0 2)Gr line corresponds to the extra graphite present in the material (about 2000 ppm). (For interpretation of the references to colour in this figure legend, the reader is referred to the web version of this article.)

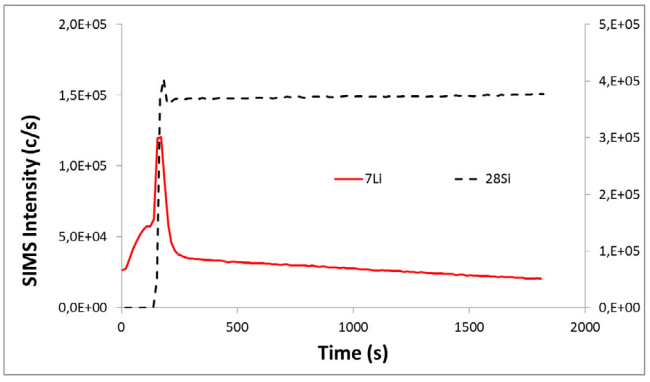


**Fig. 9.** SIMS profiles from the SiC surface in contact with the $B_4C$ disc (the scale of the dashed line is on the left, the bold line on the right).

(94%), 1.78 MeV (6%) for $^4$He respectively. When produced close to the $B_4C$ surface, they can penetrate SiC. For example, the stopping length for 1 MeV $^7$Li in SiC is about 1.8 μm. Such an implantation depth for Li is consistent with the SIMS-measured Li profile in SiC. X-ray diffraction was performed under the same conditions as for $B_4C$. This means that the analysed depth (about 7 μm) exceeds the implantation range of Li, and reveals some damage (Fig. 10). It is now known that some irradiation damage in SiC can be annealed when heated at its previous irradiation temperature [9]. When damaged by transmutation recoils, the SiC surface can be heat-treated to determine the annealing temperature of the irradiation damage that corresponds to the irradiation temperature. This remains to be done.

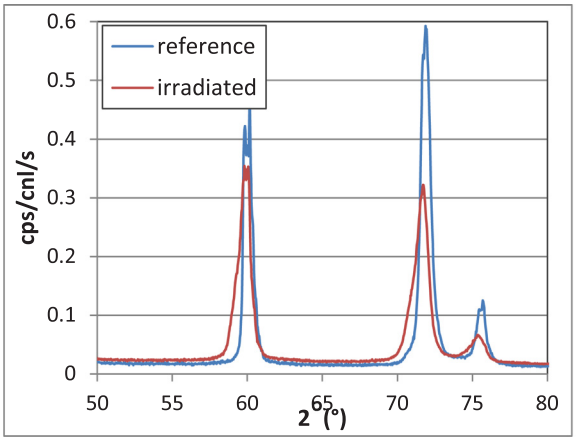


**Fig. 10.** XRD diagrams of the surface of the SiC disc in contact with the $B_4C$ disc.

## 8. Conclusion

We have proposed a new methodology to study neutron absorber materials based on the irradiation of $B_4C$ samples in a pure thermal neutron flux at the ILL reactor. The $B_4C$ samples obtained were homogeneously damaged in the bulk at a temperature that may be known in the near future. After some decay, the samples were no longer radioactive, which made them well-suited for further studies on the characterisation of transmutation damage. Our next objectives will be to analyse the structural damage in $B_4C$, to identify the possible occurrence of helium clusters, and to determine the temperature level at which transmutation damage is annealed in $B_4C$ so as to identify which of these are relevant for fast breeder reactor operating conditions. Characterisation of the $^{10}B$-enriched $B_4C$ discs that were also irradiated should provide some valuable information by way of comparison with the sample studied herein.

In addition to our scientific objectives, some technical improvements could also be made to simplify the handling of irradiated samples. The gamma dose rate of the sample holder could be reduced by using SiC instead of aluminium for the fabrication of the sample holder. And the near-surface layer observed after irradiation could be avoided by using an improved polishing procedure for $B_4C$.

## References

[1] Marjorie Bertolus, Michel Freyss, Boris Dorado, et al., Linking atomic and mesoscopic scales for the modelling of the transport properties of uranium dioxide under irradiation, J. Nucl. Mater. 462 (2015) 475–495.
[2] J.A. Basmajian, A.L. Pitner, D.E. Mahagin, H.C.F. Rippel, D.E. Baker, Irradiation effects in boron carbide pellets irradiated in a fast neutron spectra, Nucl. Tech. 16 (1972) 238–248.

[3] D. Gosset, Absorber materials, in: Dan Gabriel Cacuci (Ed.), Sodium Fast Reactor Design: Fuels, Neutronics, Thermal-Hydraulics, Structural Mechanics and Safety, Handbook of Nuclear Engineering, Springer, 2010.
[4] G.W. Hollenberg, Effect of fast neutron irradiation on the structure of boron carbide, J. Am. Cer. Soc. 60 (11-12) (1977) 520–525.
[5] A. Letourneau, et al., Annal. Nucl. Energy 33 (2006) 377–384.
[6] R. Boffy, S. Peuget, R. Schweins, et al., High thermal neutron flux effects on structural and macroscopic properties of alkali-borosilicate glasses used as neutron guide substrate, Nucl. Instum. Methods B 374 (2016) 14–19.
[7] D. Simeone, X. Deschanels, B. Berthier, C. Tessier, Experimental evidence of lithium migration out of an irradiated boron carbide material, J. Nucl. Mater. 245 (1997) 27–33.
[8] D. Gosset, D. Simeone, D. Quirion, Neutron irradiation damage of boron carbide: an X-ray diffraction evaluation, J. Phys. IV France Pr10 (2000) 55–63.
[9] J.E. Palentine, The development of silicon carbide as a routine irradiation temperature monitor, and its calibration in a thermal reactor, J. Nucl. Mater. 61 (1976) 243–253.